Proceedings Tailings and Mine Waste 2015
Vancouver, BC, October 26 to 28, 2015

Numerical model comparison on deformation behavior of a TSF embankment subjected to earthquake loading

Jorge Castillo, Yong-Beom Lee
Ausenco, USA

Aurelian C. Trandafir
Fugro GeoConsulting Inc., USA

ABSTRACT

This paper introduces two independent numerical modeling approaches used to investigate the earthquake response of a tailings embankment dam on a foundation consisting of liquefiable alluvial soil. The approaches employ non-linear two-dimensional finite-difference and finite-element numerical schemes along with fully-coupled effective stress constitutive models for liquefaction. Details of the parameters describing each liquefaction constitutive model and results of model calibration against experimental data from liquefaction cyclic triaxial tests are presented. Comparison of numerical results addressing the seismic performance of the analyzed embankment-liquefiable foundation system indicates agreement between the two independent modeling approaches in terms of predicted deformation pattern of the system and magnitude of permanent dam displacement. The study demonstrates that both considered numerical modeling approaches represent a useful and robust tool for analyzing the deformation behavior of tailings dams on liquefiable foundation under seismic conditions.

Keywords: tailings dam, liquefaction, finite-difference modeling, finite-element modeling, seismic displacements

1 INTRODUCTION

The seismic behavior of tailings storage facilities (TSFs) represents a major concern for mining projects in earthquake prone areas. TSF embankment dams founded on liquefiable soils may experience excessive displacements and eventually failure due to earthquake induced liquefaction of the foundation zone. Numerical modeling is a valuable tool for investigating the seismic performance of TSF embankments on liquefiable foundations in order to design effective mitigation strategies against liquefaction related tailings dam failure.

This paper presents two independent numerical modeling approaches that can be utilized to investigate the seismic behavior of TSF embankments founded on liquefiable soils. The approaches employ finite-difference and finite-element based numerical schemes along with advanced sophisticated constitutive models able to reproduce the complex undrained shear behavior of liquefiable soils observed in laboratory cyclic triaxial tests. An example problem is used to illustrate the ability of the considered numerical modeling approaches to reproduce large displacements likely to be experienced by a TSF embankment due to earthquake induced liquefaction of the foundation materials.

2 PROBLEM SPECIFICATION AND MATERIAL GEOTECHNICAL PROPERTIES

Figure 1 shows the geometry of the analyzed TSF embankment-foundation system along with the materials included in various components of the system. The embankment has a height of 30 m and consists of three different materials (i.e., transition fill, structural fill and waste rock or rockfill) distributed as shown in Figure 1. A liner system consisting of geomembrane and geosynthetic clay liner is considered along the upstream dam slope and at the base of the impoundment area (Figure 1). The role of the liner system is to prevent seepage from tailings

into the body of the embankment thus maintaining the embankment in unsaturated conditions. The foundation ground consists of a 10 m thick medium-dense liquefiable alluvial soil involving silty sand with gravel and underlain by bedrock (Figure 1). Groundwater table (GWT) is located at 2 m below the original ground surface (Figure 1). The embankment dam stores hydraulically deposited tailings assumed to be in a slurry state.

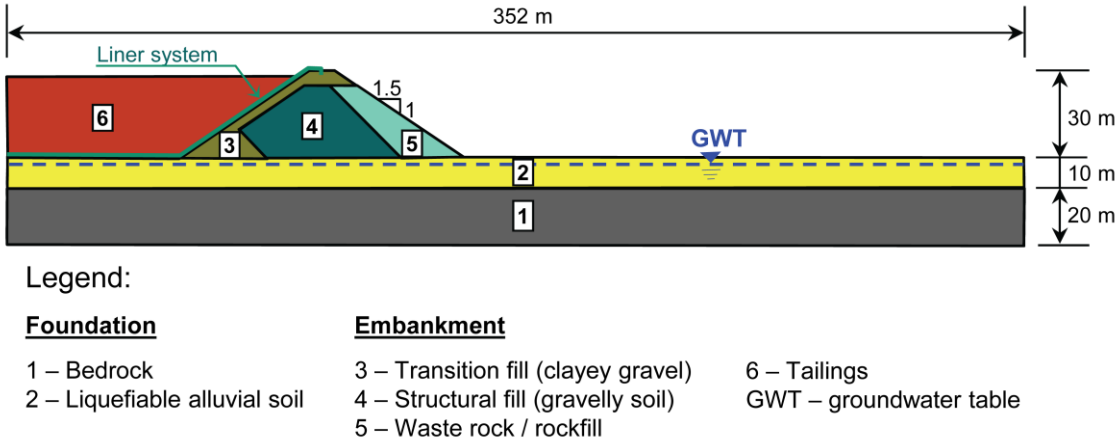

Figure 1. Geometry and materials of the analyzed TSF embankment-foundation system.

The geotechnical properties of various considered embankment and foundation materials are provided in Table 1. The elasto-plastic Mohr-Coulomb model was used to characterize the stress-strain behavior of these materials in the numerical analysis, with the exception of the liquefiable alluvial soil unit below the groundwater table which was modeled using advanced constitutive models for liquefaction available in the finite-difference and finite-element computer codes employed in this study. Descriptions of the constitutive models used to simulate the liquefaction behavior of the saturated alluvial soil, as well as the modeling approach used for tailings, are provided in the following sections of the paper. A total density of 1.73 t/m^3 was used for tailings in the numerical analysis.

Table 1. Types and geotechnical properties of embankment and foundation materials.

Material type	Density [t/m^3]	Young's modulus [kPa]	Poisson's ratio	Cohesion [kPa]	Friction angle [°]
Bedrock	2.65	2.72 x 10^6	0.200	4,000.0	36
Liquefiable alluvial soil below GWT	1.93	1.95 x 10^5	0.313	0	35
Liquefiable alluvial soil above GWT	1.85	1.95 x 10^5	0.313	0	35
Transition fill	1.89	8.59 x 10^5	0.278	0	38
Structural fill*	2.24	1.97 x 10^6	0.263	20.0	35.5
Waste rock / rockfill*	2.35	1.97 x 10^6	0.263	10.0	45.7

*In the finite-difference modeling, a secant friction angle versus effective normal stress relationship defined according to Leps (1970) was used. The relationship provides shear strength values similar to the shear strength obtained using the Mohr-Coulomb parameters summarized in the table.

3 FINITE-DIFFERENCE MODELING APPROACH

The dynamic finite-difference analysis was conducted as a non-linear elasto-plastic two-dimensional analysis with fully coupled liquefaction triggering using Fast Lagrangian Analysis of Continua (FLAC) code (Itasca, 2008). The FLAC code solves the equations of motion in explicit form in the time domain using very small time steps that allows non-linear inelastic stress strain soil behavior to be incorporated.

The saturated liquefiable alluvial soil was modeled using UBCSAND, a user defined model incorporated into FLAC. The UBCSAND model is based on the FLAC Mohr-Coulomb model and was developed by Dr. Peter M. Byrne and his colleagues at the University of British Columbia (Byrne et al., 2003; Byrne, 2009). The model simulates the stress-strain behavior of soil under static or cyclic loading for drained, undrained, or partially drained conditions by using an elasto-plastic formulation at all stages of loading rather than just at the failure state. In this way plastic strains, both shear and volumetric, are predicted at all stages of loading. The plastic parameters in the model are selected to give agreement with results from simple shear element tests, considered to most closely replicate conditions in the field during earthquake loading.

Conventional state-of-practice procedures for evaluating liquefaction use separate analyses for liquefaction triggering, displacement, and flow slides. These conventional procedures are not capable of predicting the generation of excess pore-water pressure, dynamic response, and displacement patterns simultaneously. The UBCSAND model is a fully coupled effective stress procedure enabling the dynamic response in terms of pore pressures, accelerations and displacements caused by a specific input seismic motion. In this manner liquefaction triggering, deformation and flow slide potential are evaluated in a single integrated analysis.

Figure 2 shows the FLAC grid of analyzed TSF embankment-foundation system. The mesh size for the FLAC model was selected to provide accurate seismic wave transmission. The tailings were assumed to be fully liquefied and were modeled as an applied pressure to the upstream face of the dam. This neglects the shear strength of the tailings prior to the onset of liquefaction as well as the nominal post-liquefaction shear strength and adds conservatism to the results. This simplifying assumption was made to avoid adding an excessive number of elements in the model that would increase computational time.

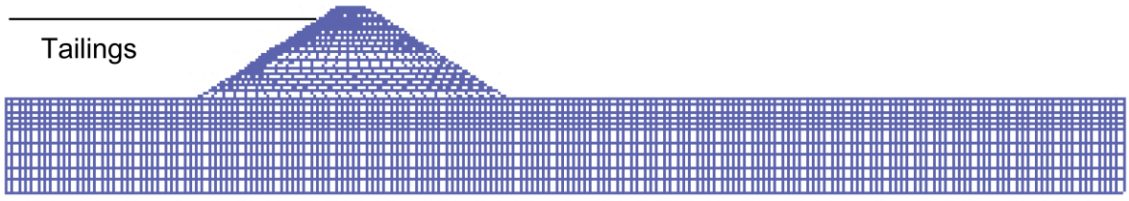

Figure 2. FLAC grid of analyzed TSF embankment-foundation system.

The UBCSAND model implementation in FLAC was calibrated initially by selecting the $(N_1)_{60}$ value that matches the results of cyclic triaxial testing conducted on saturated liquefiable alluvial soil samples subjected to initial effective consolidation stresses of 90 kPa and 300 kPa. In the UBCSAND calibration the cyclic triaxial test results were reduced by applying a factor of 2/3 to represent comparable in situ stress conditions (Idriss and Boulanger, 2008). The model calibration was accomplished by using a single element simulation in FLAC to model the laboratory tests. The single element was assigned elastic and plastic parameters based on a $(N_1)_{60}$ value as described by Byrne et al. (2003). Plastic modification factors were also applied to calibrate UBCSAND model to experimental data. Table 2 shows the parameters of the UBCSAND model for the saturated liquefiable alluvial soil.

Based on a comparison of the predicted number of cycles to liquefaction and the measured number in the laboratory tests, the $(N_1)_{60}$ was adjusted if necessary and the simulation repeated until the predicted and measured number of cycles were approximately the same. As shown in Figure 3, for $(N_1)_{60}$ =12 the calibration curve generated by UBCSAND fits the actual triaxial test (TX) data quite well (see solid lines in Figure 3). The model was also calibrated using the converted triaxial cyclic stress ratio (CSR) values to represent values from cyclic simple shear (SS) test and more accurately reflect in situ stress conditions (dotted line in Figure 3).

Table 2. Parameters of the UBCSAND constitutive model for saturated liquefiable alluvial soil

	Plastic modification factors			
$(N_1)_{60}$	*m_hfac*1	*m_hfac*2	*m_hfac*3	*m_hfac*4
12	0.7	0.3	0.2	0.5

The model parameters summarized in Table 2 are briefly introduced in the following:

- $(N_1)_{60}$ is the corrected standard penetration resistance;
- *m_hfac*1 is a primary hardener parameter controlling the number of cycles to trigger liquefaction;
- *m_hfac*2 is a secondary hardener parameter used to refine the shape of the pore pressure increase with the number of cycles;
- *m_hfac*3 represents a dilatancy hardener controlling the liquefaction post-triggering response;
- *m_hfac*4 is a parameter used to reduce dilatancy after liquefaction triggering.

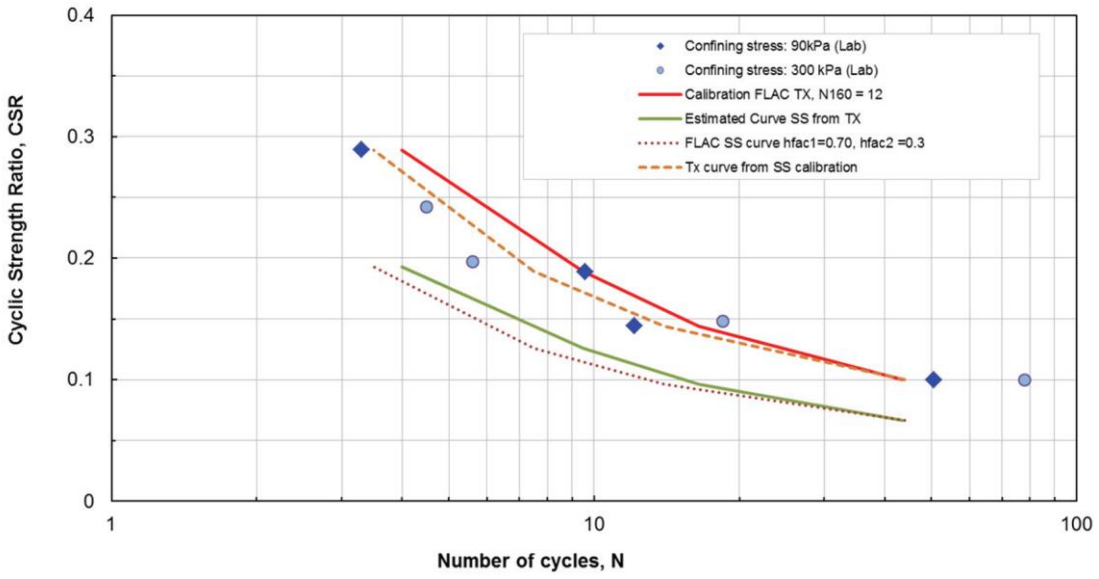

Figure 3. Experimental and UBCSAND model predicted liquefaction resistance of the considered liquefiable alluvial soil.

Figures 4(a) and 4(b) show the UBCSAND calibration against the laboratory data for the shear stress ratio vs. number of cycles, and excess pore pressure ratio vs. number of cycles for a sample with a confining stress of 90 kPa. In general, there was a good agreement between the model and laboratory testing.

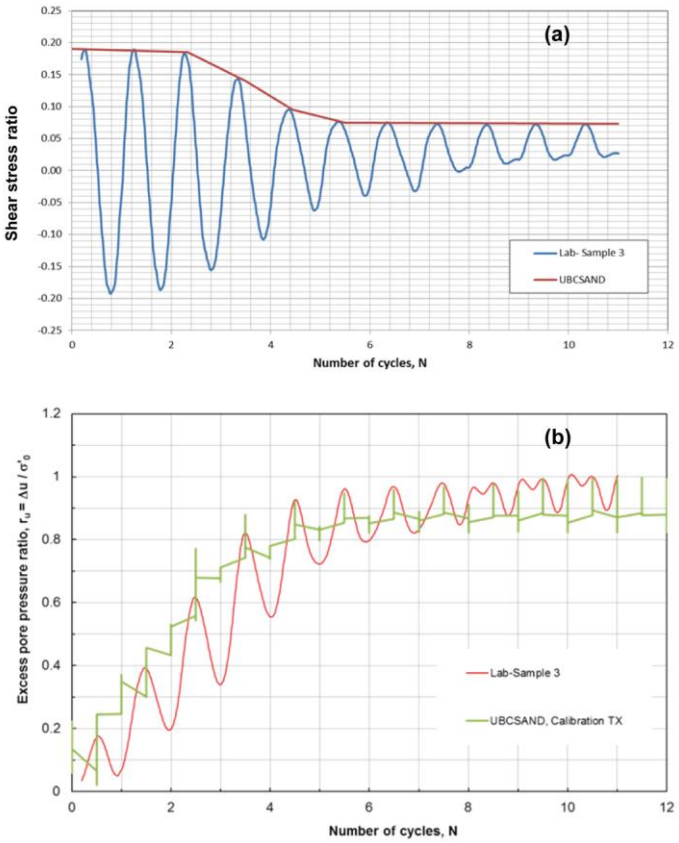

Figure 4. Example of experimental and UBCSAND model simulated behavior of the considered liquefiable alluvial soil: (a) shear stress ratio vs. number of cycles, and (b) pore pressure ratio vs. number of cycles.

4 FINITE-ELEMENT MODELING APPROACH

The dynamic finite-element analysis of the TSF embankment-foundation system was conducted using the finite-element based numerical scheme developed and described by Wakai and Ugai (2004) along with a generalized plasticity constitutive formulation required for effective stress based fully-coupled undrained shear behavior modeling of the saturated liquefiable alluvial soil. Figure 5 shows the mesh of the analyzed TSF embankment-foundation system considered for the finite-element modeling approach. The finite-element model consists of 676 isoparametric elements involving eight - noded and six - noded quadrilateral and triangular element configurations, respectively. The model has a total horizontal length of 352 m and a maximum height of 60 m measured from the model bottom boundary to the crest of the embankment (Figure 1).

The boundary conditions of the finite-element model for dynamic analysis involved restrained horizontal and vertical relative displacements along the bottom boundary where the input ground motion was applied, and absorbing (viscous) boundaries along the vertical edges to ensure appropriate dissipation of the outward propagating seismic waves. The dynamic finite-element analysis employed the initial stresses obtained from a static finite-element analysis that involved activation of the gravitational loads in the system. Tailings were modeled as a zero shear strength material in order to achieve loading conditions on the upstream face of the embankment and the upstream portion of the original ground surface similar to the tailings

related loads applied in the finite-difference modeling approach described in the previous section.

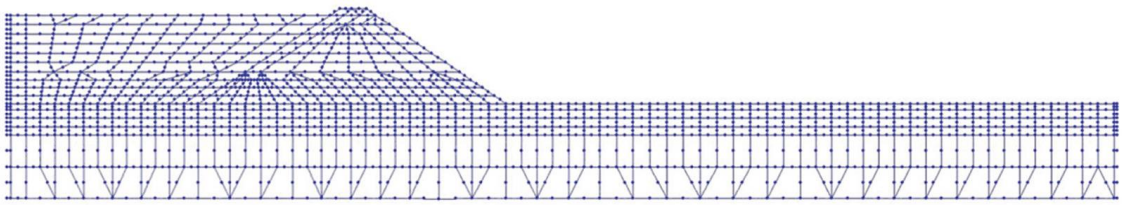

Figure 5. Finite-element mesh of the analyzed TSF embankment-foundation system.

The dynamic shear behavior of the saturated liquefiable alluvial soil from the foundation (Figure 1) was modeled using the Pastor-Zienkiewicz constitutive formulation (Pastor et al., 1990) referred herein to as PZ model. The PZ model employs a generalized plasticity framework which enables a rigorous characterization of the saturated soil shear behavior under static and cyclic loading conditions. The model is defined by fifteen parameters summarized in Table 3 and briefly introduced in the following:

- G_{es0} and K_{ev0} are constants in the expressions of shear modulus and bulk modulus describing the elastic behavior;
- m_s and m_v are shear modulus and bulk modulus exponents, respectively;
- M_g and γ_g are parameters describing the direction of the plastic flow vector;
- M_f and γ_f are parameters describing the direction of the load vector normal to the yield surface;
- C is the ratio between the critical state stress ratio in extension (M_e) and the critical state stress ratio in compression (M_c), from triaxial tests;
- H_0, γ_0, γ_1 and α are parameters describing the plastic modulus during loading;
- H_{U0} and γ_U are parameters describing the plastic modulus during unloading.

Table 3. Parameters of the PZ constitutive model for saturated liquefiable alluvial soil.

G_{es0}	K_{ev0}	m_s	m_v	M_g	γ_g	M_f	γ_f	C	H_0	γ_0	γ_1	α	H_{U0}	γ_U
422	234	0.5	0.5	1.7	0.45	0.8	0.45	0.9	700	4.7	0.19	7.0	7,000	3.4

The PZ model parameters provided in Table 3 were calibrated using results from laboratory undrained cyclic triaxial tests conducted on isotropically consolidated saturated liquefiable alluvial soil samples subjected to initial effective consolidation stresses of 90 kPa and 300 kPa. A loading frequency of 1 Hz was used in the laboratory cyclic triaxial tests. Results showing experimental and PZ model simulated behavior of the liquefiable alluvial soil in the cyclic triaxial tests are presented in Figures 6 and 7. Figure 6 shows a good agreement between experimental and PZ model predicted liquefaction resistance of the liquefiable alluvial soil. As seen in Figure 7, the calibrated PZ model is able to accurately reproduce the excess pore pressure generation pattern in relation to the number of applied loading cycles and onset of large plastic axial strains representative of liquefaction triggering observed in the laboratory cyclic triaxial tests. Liquefaction in cyclic triaxial tests was assumed to occur when the mean effective stress attained a zero value (i.e., the excess pore pressure ratio, defined as the excess pore pressure divided by the initial effective consolidation pressure, reached 100%) or when a double-amplitude axial strain of 5% was attained, whichever occurred first.

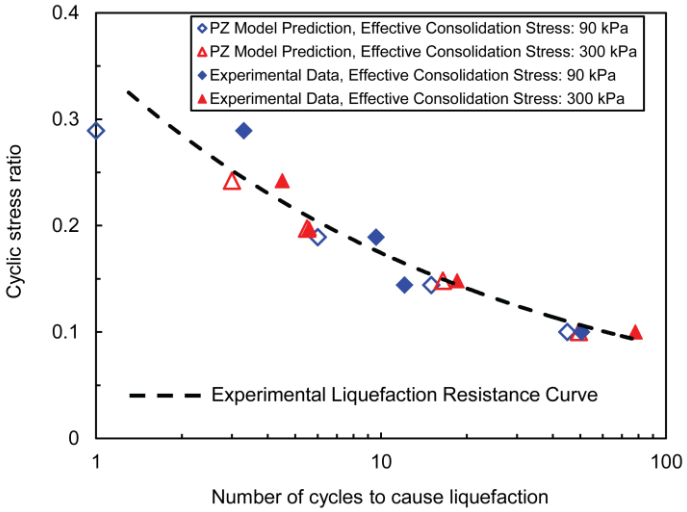

Figure 6. Experimental and PZ model predicted liquefaction resistance of the saturated liquefiable alluvial soil.

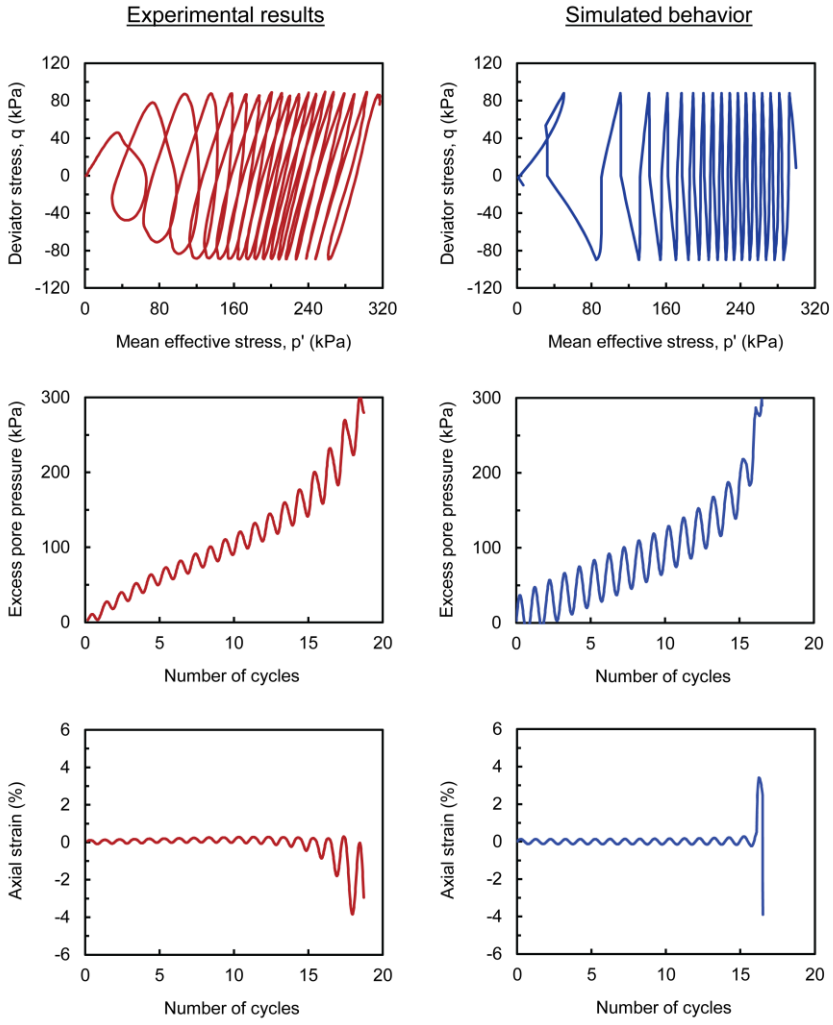

Figure 7. Example of experimental and PZ model simulated behavior of the saturated liquefiable alluvial soil in the cyclic undrained triaxial test in terms of effective stress path, and excess pore pressure and axial strain evolution in relation to number of cycles.

5 COMPUTATIONAL RESULTS

The dynamic deformation analysis of the TSF embankment-foundation system was conducted for an input base excitation described by the acceleration time history with a peak acceleration of 0.1*g* (where *g* represent the gravitational acceleration) presented in Figure 8. It is noteworthy that the finite-difference modeling approach requires the input base excitation to be specified in the form of velocity time history obtained by integrating the acceleration time history from Figure 8, whereas the finite-element modeling approach takes the input base excitation directly in the form of acceleration time history.

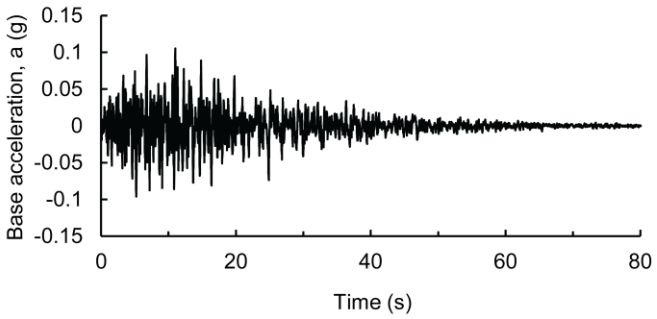

Figure 8. Acceleration time history of the input base excitation.

Results from dynamic FLAC and finite-element analyses are presented in Figures 9 and 10, respectively, in terms of deformed finite-difference grid and finite-element mesh at the end of the earthquake and evolution of computed horizontal and vertical displacements of the upstream edge of the crest of the embankment identified as point A in the figures. Both numerical modeling approaches show a similar computed deformation pattern of the embankment-foundation system along with agreement in calculated permanent downstream horizontal and downward vertical displacements at point A, of 2.2 m and 0.1 m from the FLAC analysis (Figure 9) and 2.8 m and 0.6 m from the finite-element analysis (Figure 10).

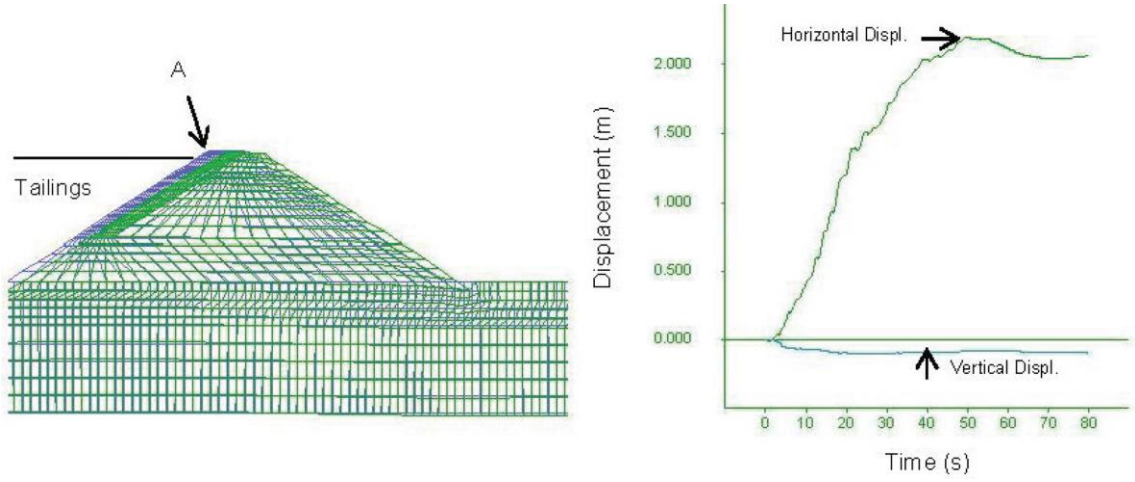

Figure 9. Original and deformed grid of the FLAC model, and computed time histories of horizontal and vertical displacements of the upstream edge of the crest of the embankment.

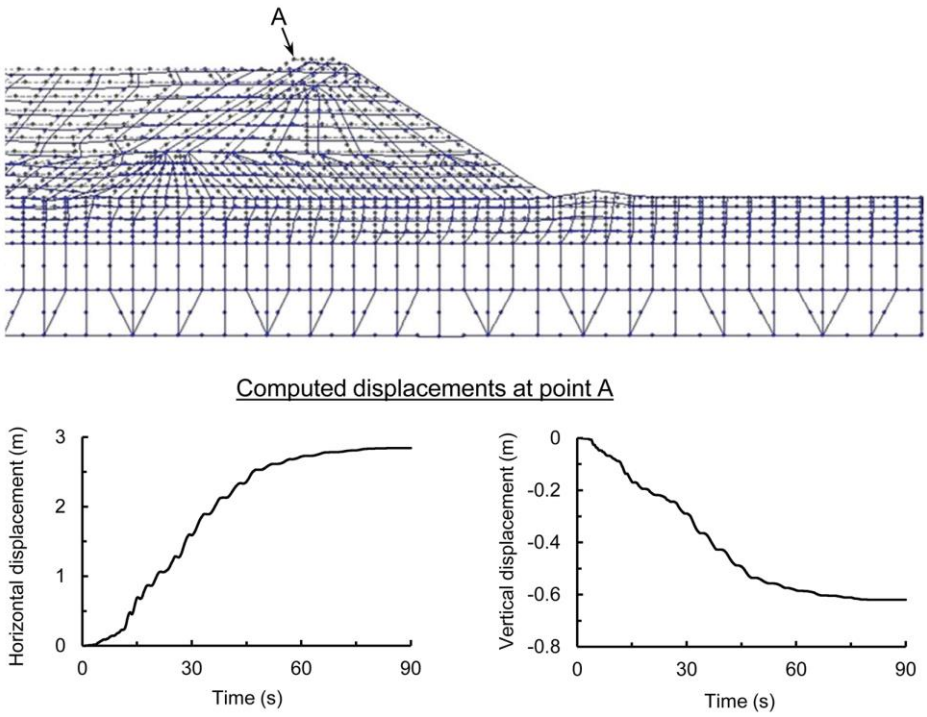

Figure 10. Original and deformed finite-element mesh at the end of the earthquake, and computed time histories of horizontal and vertical displacements at the upstream edge of the crest of the embankment.

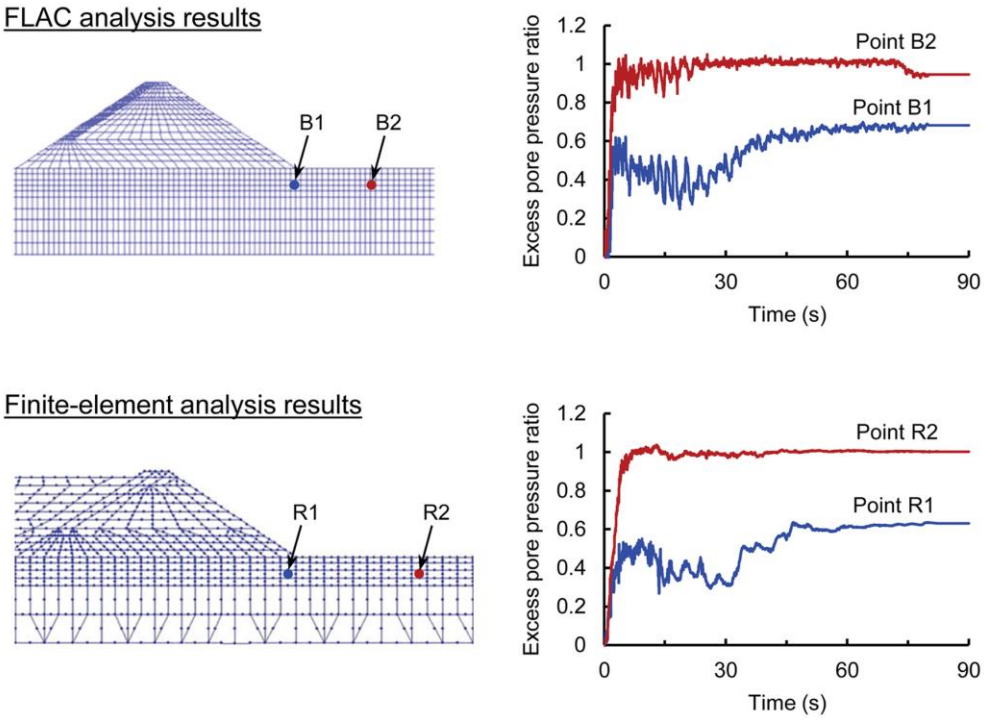

Figure 11. Computed time histories of the excess pore pressure ratio at the middle of the saturated alluvial soil unit beneath the downstream toe of the embankment and in the far field.

The large lateral displacement of the embankment occurs due to large lateral deformation of the saturated alluvial soil in the foundation as a result of earthquake induced liquefaction. The predominantly lateral migration of the foundation soil towards the free field is illustrated by the pronounced distortion of the portion of the finite-difference grid and finite-element mesh comprising the saturated liquefiable alluvial soil and associated bulging of the foundation soil adjacent to the downstream toe of the embankment (Figures 9 and 10).

Figure 11 shows agreement in computed excess pore pressure ratio by the two independent numerical modeling approaches at the middle of the saturated alluvial soil unit beneath the downstream toe of the embankment and in the far field. A drop in excess pore pressure response beneath the downstream toe can be observed in Figure 11, starting at an elapsed time of about 8-11 s and reflecting a dilative behavior associated with bulging of the foundation soil adjacent to the toe (Figures 9 and 10). This decay in excess pore pressure prevented the alluvial soil underneath the toe of the dam to attain a final excess pore pressure ratio of 1.0.

A threshold value of the excess pore pressure ratio of 0.7 was used to distinguish between liquefied and non-liquefied foundation zones in the present numerical analysis. As seen in Figure 12, both numerical modeling approaches predicted the occurrence of a non-liquefied zone (i.e., excess pore pressure ratio less than 0.7) of relatively similar extent within the saturated alluvial soil beneath the downstream slope of the embankment.

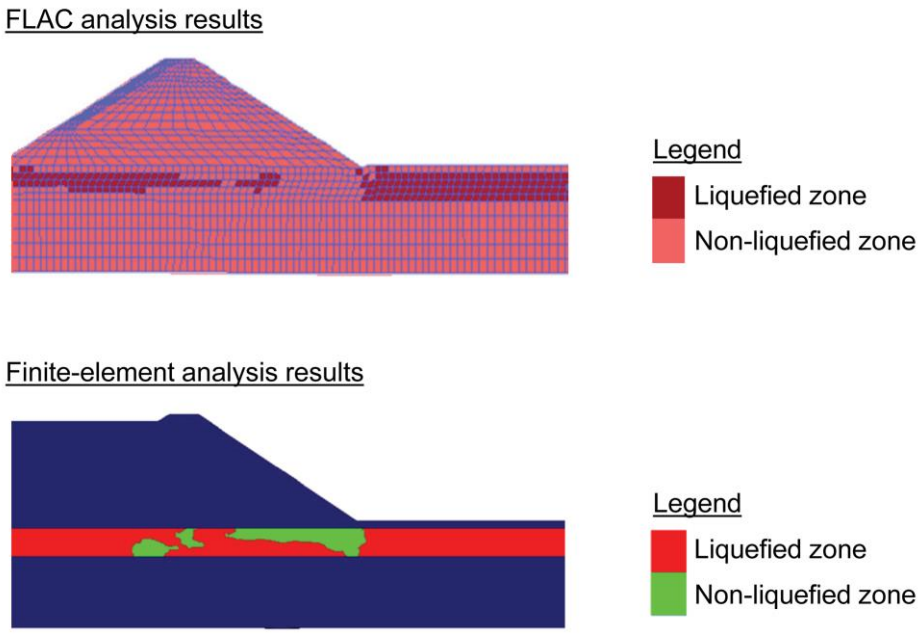

Figure 12. Computed distribution of liquefied and non-liquefied zones within the saturated alluvial soil unit.

6 CONCLUSIONS

The numerical analysis results presented in this paper demonstrated the capability of the considered finite-difference and finite-element modeling approaches to accurately reproduce the undrained shear behavior of liquefiable soils under cyclic loading and to assess the impact of earthquake induced liquefaction of foundation soils on permanent displacements of TSF embankment dams. For the analyzed TSF embankment-foundation system and considered characteristics of the input ground motion, the numerical outcomes from finite-difference and finite-element analyses are not significantly different and the results reveal the level of uncertainty that may be expected when applying different sophisticated constitutive models for liquefaction to full-scale studies. Such modeling approaches can be employed to investigate the effectiveness of various potential remedial measures (e.g., buttress fill, foundation improvement, etc.) in mitigating excessive displacements that may be experienced by embankment dams on liquefiable foundation soils during an earthquake.

7 REFERENCES

Byrne, P.M., Park, S.S., & Beaty M. 2003. Seismic liquefaction: centrifuge and numerical modeling. *FLAC and Numerical Modelling in Geomechanics-2003*, Proceedings of the 3rd International FLAC Symposium, , R. Brummer et al. (eds), Sudbury, Ontario, Canada: 321-331. Lisse: Balkema.

Byrne, P.M. 2009. Professor Emeritus at the University of British Columbia, Civil Engineering Department. Personal communication.

Idriss I.M., & Boulanger, R.W. 2008. Soil Liquefaction during Earthquakes. *Earthquake Engineering Research Institute*, MNO-12, Oakland, California, USA.

Itasca 2008. *Fast Lagrangian Analysis of Continua*, Version 6.0. Itasca Consulting Group, Inc.

Leps, T.M. 1970. Review of shearing strength of rockfill. *Journal of the Soil Mechanics and Foundations Division*, ASCE, 96 (4): 1159–1170.

Pastor, M., Zienkiewicz, O.C., & Chan, A.H.C. 1990. Generalized plasticity and the modelling of soil behaviour. *International Journal for Numerical and Analytical Methods in Geomechanics* 14 (3): 151–190.

Wakai, A., & Ugai, K. 2004. A simple constitutive model for the seismic analysis of slopes and its applications. *Soils and Foundations* 44 (4): 83–97